

DIRECT DETECTION OF SMALL MOTION FROM DYNAMIC COMPUTED TOMOGRAPHY IMAGES

Jean-Philippe Thiran

Shima Sepehri

Signal Processing Laboratory (LTS5)
Swiss Federal Institute of Technology
Lausanne (EPFL)
EPFL STI IEL LTS5, Station 11
1015 Lausanne, Switzerland

Signal Processing Laboratory (LTS5)
Swiss Federal Institute of Technology
Lausanne (EPFL)
and Department of Radiology
University Hospital Center (CHUV)
and University of Lausanne (UNIL)
EPFL STI IEL LTS5, Station 11
1015 Lausanne, Switzerland

ABSTRACT

In this paper, we present a new and precise method to detect small motions directly from the raw data of the X-ray scan, called sinograms. The application for which the method has been developed, namely the detection of the wall motion of intracranial aneurysm, will be presented and the required verification process will be showed with results. This direct motion detection method has the advantage of eliminating any unnecessary calculation, by directly using the sinograms, instead of the reconstructed image. Such error elimination is particularly important in critical applications, like the medical diagnostics, and for small motions, such as the motion of the wall of a body organ. The performance of the method is evaluated by comparison with digital and physical phantoms.

Index Terms— direct detection, sinogram, B-spline deformation, small motion, intracranial aneurysm, Computed Tomography (CT) scan

1. INTRODUCTION

Detection of motion of the objects inside an opaque body, in a noninvasive way, like through an X-ray scan, have many applications, such as medical diagnostics. One of the most precise and common dynamic medical image modalities is the four dimensional CT scan. This process reconstruct the three dimensional body at different time instances and by seeing the sequence of the three dimensional volumes through time the motion can be detected.

However, the mathematical reconstruction process is prone to many inevitable calculation errors, even with the best methods. In fact, the reconstructed images are prone to

known ring like artefacts, due to the lack of calibration, or limited resolution, and the partial volume effect [1, 2]. Since the motion of the object is reflected in the raw data of this process, the footprint of the X-ray, we proposed a less error-prone framework to detect the motion directly from these raw data and therefore eliminate any unnecessary error coming from the image reconstruction process.

For the validation, we developed a digital and also a physical phantom to exactly measure the error of the algorithm in order to make it usable for very critical applications, such as the medical diagnostics.

1.1. Sinogram of a Moving Object

A sinogram is a visual representation of the raw data obtained in a CT scan. Consider an object through which the X-ray is passing, as shown in Fig. 1. As we see in this image, the deformation of an object which affects the amount of absorption of the X-ray $P(t)$ is reflected in the sinogram. This is important, because the sinogram is the raw data collected by a CT machine and does not feature the processing errors. Therefore, we hypothesize that the detection of small motion is more logical to be derived from these first-hand data.

2. THE MOTION DETECTION METHOD

B-splines are known to be good parameter representatives of small deformation, such as that of the wall of intracranial aneurysm, as witnessed during surgeries and dynamic imaging, and also as quantified by some studies, [1], to be, for example, maximum two pixels, or less than a millimeter (mm). Therefore, we decided to model the deformation of the object due to the motion with a cubic B-spline. More explicitly, we can consider a referenced image to be deformed, as in Fig. 2.

Research supported by the European Commission FP7 framework Program under grant FP7-ICT-2009-6- 269966 (Thrombus).

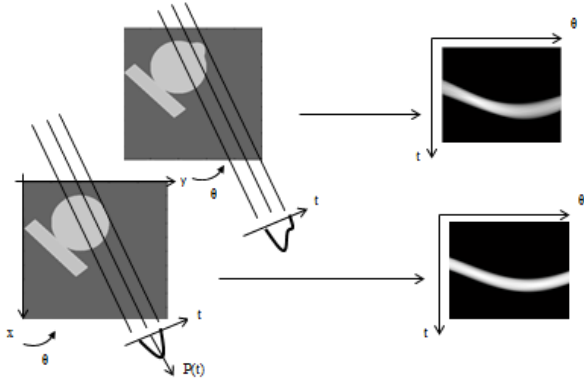


Fig. 1. The deformation of the image is reflected in the sinogram.

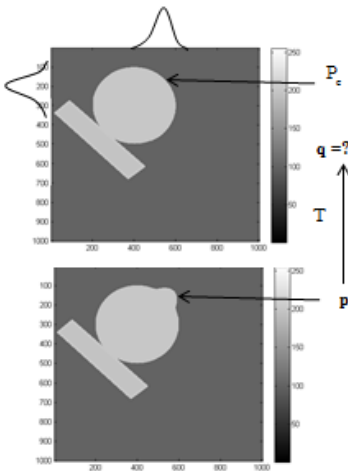


Fig. 2. The image deformation

Every point \vec{p} on the deformed image can be found using the following formula [1].

$$\mathbf{q} = \mathbf{p} + \sum_c \beta \left(\frac{\mathbf{p} - \mathbf{p}_c}{\delta_c} \right) \omega_c \quad (1)$$

where β is the tensor product of two (or three in case of a 3-D image) 1-D cubic B-splines, \sum_c is the summation on all the splines each centered around a control point \mathbf{p}_c , δ_c and ω_c are respectively the width and the parameters (here the amplitude) of each B-spline. The 1-D cubic B-splines, such as those in Fig. 2 are defined as

$$\beta^3(x) = \begin{cases} \frac{2}{3} - \frac{1}{2}|x|^2(2 - |x|) & 0 \leq |x| < 1 \\ \frac{1}{6} - (2 - |x|)^3 & 1 \leq |x| < 2 \\ 0 & \text{otherwise} \end{cases} \quad (2)$$

Using this deformation, we can now define our motion detection system. The general scenario is shown in Fig. 3

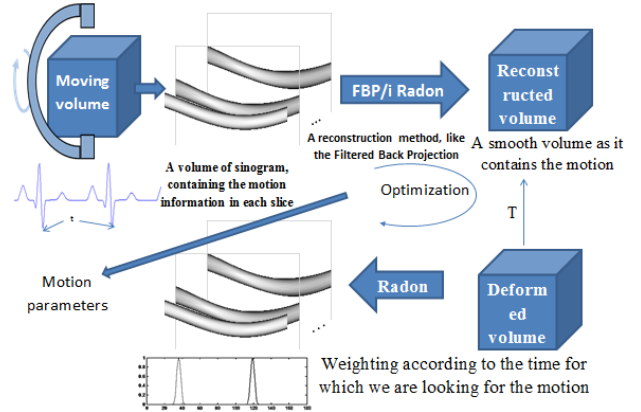


Fig. 3. The motion detection general scenario

As we see in this figure, the real volume is scanned with an X-ray scanner. The resulting sinogram is the raw data. This data is used to reconstruct a reference volume which is used for the motion detection. Unlike the classical approach in 4D ECG-Gated CT angiography, only one volume is produced from all the data, and therefore we only have once the reconstruction errors. This reference volume is blurred because while recording the sinogram the object has moved. In order to find the motion of a certain moment t of the cardiac cycle, the reference image is deformed using the B-spline model of equation 1. Then, the sinogram of this deformed volume is matched with the raw sinogram multiplied by a window centered around the desired time t . The windowing used here first acts as the extraction of the corresponding sinogram from the raw sinogram, resulted from all the motion states. Moreover, this window is a kind of regularization which relates the motion of each time state with that of the neighboring instants. The process of deforming the reference volume and matching the sinograms of the original and the deformed volumes continues in an optimization process to find the best parameters (\mathbf{p}_c, ω_c) that describe the deformation of the moving volume.

It should be taken into consideration that the first simulations, mentioned here, are used for the sensitivity analysis, (a paper in progress). This can justify the use of the same basis functions in the simulations as the ones used in the detection method, and also the reporting of the error in pixels (not mm, for example). To clarify, it should be mentioned that, unlike potential expectations that might consider reporting the results -in the next section- using physically meaningful units, such as maximum error in mm, here, we report the error in pixels. The reason is that different voxel sizes, according to different scan scenarios, can be assigned to the simulation.

3. SIMULATION RESULTS

The challenge of finding the exact motion for medical applications, to the best of our knowledge, faced a lack of quanti-

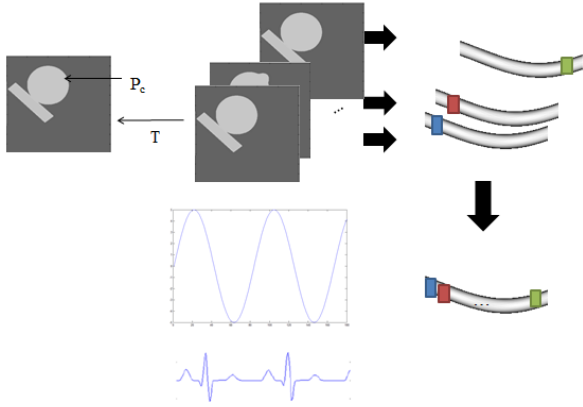


Fig. 4. The simulation image

fied validation. In other words, considering the small size of the motion and different computational errors, no value can be reliable, unless it is exactly validated. To this end, we developed a digital phantom [3] to which we can apply realistic analytical motion models and compare the values found by the algorithm with the a priori known motion models.

To explain, let us consider Fig. 4. To simulate the moving object, we consider a reference image or volume (the left-hand side image) and apply a motion model with known B-Spline parameters to a point on the wall of the aneurysm. To simulate a wall motion correlated with the heart beat, we considered a set of motions, with a varying amplitude for the B-splines, where this varying amplitude was defined, in correlation with the Electrocardiograph (ECG), to simulate the effect of the heart beat on the aneurysm wall. For example we can consider a sinusoid with its peaks corresponding to the ECG. The amplitude of each instant of this sinusoid will be the amplitude of the B-spline parameters for the motion applied to the reference image, at a different time.

Next, we produce the sinograms of the object at different motion states or time instances (on the right). However, the sinogram which is registered by a real machine is composed of different parts of different sinograms, according to the time instant. Therefore, here, in our simulation of the real scan machine, the corresponding parts of different sinogram are put together to make the final raw sinogram, as a simulation of the one described in Fig. 3. This is, in fact, to save the sinogram of the moving object exactly as it is registered by real machines. To produce the sinograms, in our simulations, the `radon` function of MATLAB[®] was used.

We also added random noise to the sinogram as the simulation of the real machine errors in registering the data by the sensors. The results are shown in Fig. 5, for a low contrast image between the object and the background, for $t = 602$ ms (nearly at the peak of the sinusoid of Fig. 4), considering a cardiac cycle of 1000 ms. As seen in this image, at the initial deformation we were quite far from the correct deformation at the desired instance, while after the deformation we are ac-

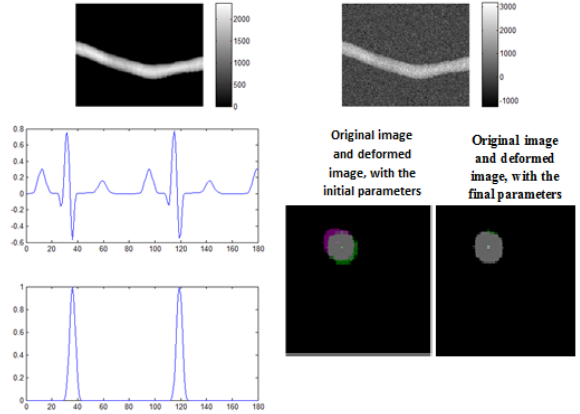


Fig. 5. The result of the simulation. Top left, the sinogram of the moving object, top right, the noisy sinogram, bottom left, the ECG and the corresponding window around the desired time, bottom right, the result of matching (left, with the initial deformation and right with the final deformation). The two colors show the pixels that are present in one of the two over-lapped images. Therefore, we see that the algorithm succeeded at finding the parameters close to the real ones.

ceptably close to the real image at time t .

The size of the windows (here Gaussian) explained in section 2 is a trade-off between the amount of error introduced in the calculation and the smoothing or the amount of extra information required.

The tests on different angles showed that although we can find the correct results, by choosing an appropriate window, the convergence is faster in the angles where we see less of the difference of the images. The same reduction of the effort was also observed when we provide more information using a larger window.

The interest of this method is that due to asynchronous ECG and rotation cycles, we gather the information of the motion of the same moment of the cardiac cycle, at different angles, as shown in Fig. 5.

In the following, we demonstrate the performance of the algorithm by error quantification, in some of the possible scenarios tested with the simulator.

3.1. Finding the Motion Parameters Without the Noise

We first validated our algorithm, using this simulator. Fig 6 shows an example of the validation of the algorithm on the simulator. It shows perfect match between the deformed image found by the algorithm and the real deformed image. This figure shows two images with the overlapped regions in white and the areas present in one object and not in the other, with different colors. Not only the deformed images are the same, but also the good correspondence of the found motion parameters and the real motion parameters are summarized in Table

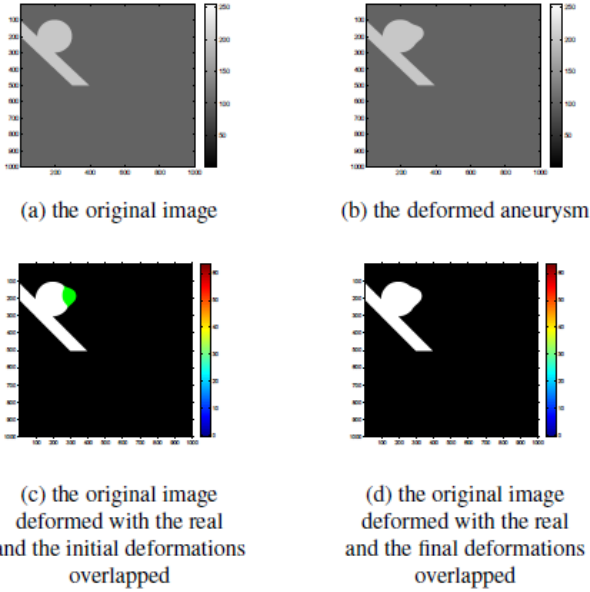


Fig. 6. Example of the performance of the algorithm with 1 control point and the search on 1 point. The green pixels show the difference between the deformed image with the a priori known motion parameters and the one deformed with the initial parameters.

<i>1 Control Point, Search on the Same Point, Exact Result</i>	
$x = 186 \text{ pixels } (p)$	$y = 299 \text{ pixels } (p)$
initial amplitude = -416 p	found amplitude = 250 p

Table 1. The result of the validation of the algorithm with the deformation applied on one control point and the results searched on the same point. Real value of the B-spline amplitude is 250.

1. For the motion of the aneurysm, we used one 2D cubic B-Splines centered at one control point on the bulb with symmetrical amplitudes.

Fig 7 and Table 2 show the good performance of the algorithm when we also add the point to which the deformation is applied as unknown parameters to be found by the algorithm.

The more realistic validation was to define a motion on a special control point and search on nearby but not exact points. This means that the real motion which was produced by applying a motion model to a special point in reality is searched by the algorithm as a sum of motions applied to nearby non-exact points. This is what will most likely happen in real acquisitions because of the quantization errors.

Fig 8 and Table 3 show the result of this validation test, with one control point, and the results searched on two neighboring pixels, from which none is the exact control point.

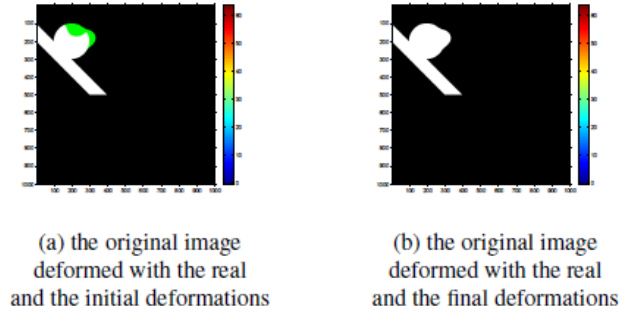


Fig. 7. Example of the performance of the algorithm with 1 control point and the search on a grid. The green pixels show the difference between the deformed image with the a priori known motion parameters and the one deformed with the initial parameters.

<i>1 Control Point, Search on a Grid, Exact Result</i>	
initial amplitude = -500 p	found amplitude = 250 p
initial x = 130 p	found x = 186 p
initial y = 220 p	found y = 299 p

Table 2. The result of the validation of the algorithm with the deformation applied on one control point and the results searched on a grid around that point. The real values of the amplitude of the B-spline and the coordinates of the control points are 250, (186,299).

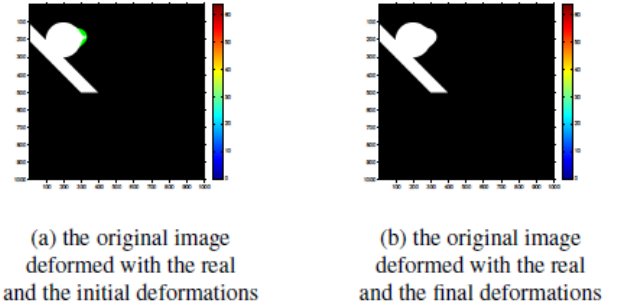


Fig. 8. Example of the performance of the algorithm with 1 control point and the search on a grid without the exact point

<i>1 Control Point, Search on a Grid, Exact Result</i>			
$x = 186 \text{ p}, y = 299 \text{ p}, \text{amplitude} = 250 \text{ p}$			
$xI(p)$	$yI(p)$	$\text{initial amplitude}(p)$	$\text{final amplitude}(p)$
186	298	130	125
186	301	130	120

Table 3. The result of the validation of the algorithm with the deformation applied on one control point and the results searched on a grid around that point.

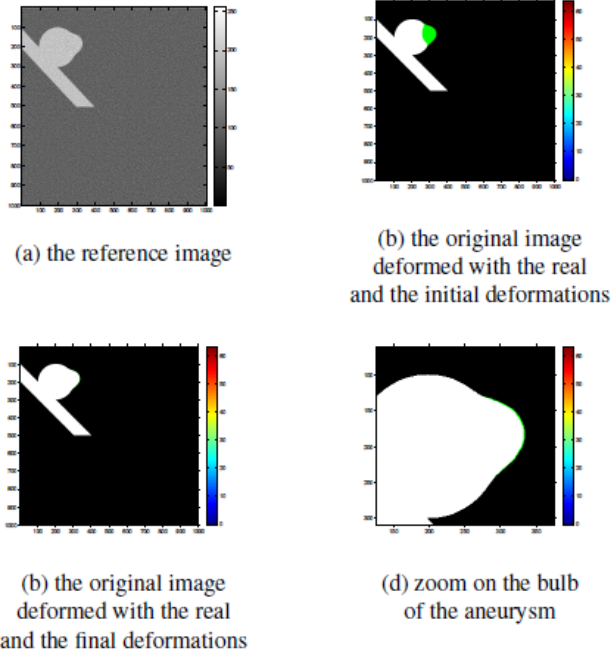


Fig. 9. Example of the performance of the algorithm with added noise (here 60 Watts) to the sinogram.

<i>1 Control Point, Search on the Same Point, Error $\leq 0.2\%$</i>	
$x = 186$ and $y = 299$	
<i>PSNR in dB</i>	<i>found amplitude (p)</i>
40	248
60	251
80	249

Table 4. The result of the validation of the algorithm with White Gaussian Noise. The initial and the real values of the B-spline amplitude are -416 and 250, respectively.

3.2. Finding the Motion Parameters with Added Noise

By the addition of the white Gaussian noise as a simulation of the noise in registering the data by the sensors, we have the following results depicted in Fig 9 and Table 4.

It was observed that with high noise power, where the reconstructed images are of very bad qualities, and therefore it is impossible to detect the motion from them, our algorithm shows a very good performance with respect to the ground-truth.

4. CONCLUSION AND FUTURE WORK

We presented a methodology to detect the motion of a moving object under the imaging process, directly from the raw data.

The performance of the algorithm was shown by error quantification achieved by the use of a digital phantom.

<i>1 Control Point, Search on a Grid with the Same Point , Error (of the maximum motion point) $< 5\%$</i>			
$x = 186$ and $y = 299$			
<i>PSNR in dB</i>	<i>found amplitude</i>	<i>found x</i>	<i>found y</i>
50	201	187	299
60	209	187	299
80	233	185	298

Table 5. The result with the added noise and the search on a grid of points. The initial and the real values of the B-spline amplitude are -500 and 250, respectively.



Fig. 10. The phantom model for validation

In a near future, we will validation this algorithm with a realistic phantom, as shown in Fig. 10. It is made of a silicon tube with the realistic sizes according to the literature. A pulsatile liquid flow controlled with computer is in the system, resulting in a pulsatile aneurysm. This system will be next imaged using a CT scan and the raw sinograms, in comparison with the ground truth motion values detected by a high quality camera, and is used to validate the algorithm.

5. REFERENCES

- [1] C. Zhang, M. Villa-Uriol, M. De Craene, J.M. Pozo, and A.F. Frangi, "Morphodynamic analysis of cerebral aneurysm pulsation from time-resolved rotational angiography," *IEEE Transactions on Medical Imaging*, vol. 28, no. 7, pp. 1105–1116, July 2009.
- [2] L.A Feldkamp, L.C. Davis, and J.W. Kress, "Practical cone-beam algorithm.," *Journal of the Optical Society of America*, vol. 1, no. 6, pp. 612–619, 1984.
- [3] Sh. Sepehri, K. Zouaoui, and J-Ph. Thiran, "A realistic computed tomography sinogram simulator for small motion analysis of cerebral aneurysms," Accepted for the 35th Annual International Conference of the IEEE Engineering in Medicine and Biology Society, 3 - 7, July, 2013.